ImmunoTargets and Therapy

Dovepress
Taylor & Francis Group

Open Access Full Text Article

ORIGINAL RESEARCH

PD-L1/ITGB4 Axis Modulates Sensitivity of Hepatocellular Carcinoma to Sorafenib via FAK/AKT/mTOR Signaling Pathway

Tao Zhu[1,*], Niandie Cao[1,*], Li Tu[1,*], Shiqi Ouyang[1,*], Zengli Wang[1,*], Yong Liang[2], Shuping Zhou[3], Xiaolong Tang[1,3]

[1]Medical School, Anhui University of Science and Technology, Huainan, People's Republic of China; [2]Central and Clinical Laboratory, Affiliated Huaian Hospital of Xuzhou Medical University, Huaian, People's Republic of China; [3]Department of Hepatology, First Affiliated Hospital, Anhui University of Science and Technology, Huainan, People's Republic of China

*These authors contributed equally to this work

Correspondence: Yong Liang; Xiaolong Tang, Email yongl@xzhmu.edu.cn; xltang2006@aust.edu.cn

Background: Hepatocellular carcinoma (HCC) frequently develops resistance to sorafenib, a first-line treatment for advanced HCC. While PD-L1 contributes to immune evasion and direct tumor survival, its role in modulating sorafenib resistance via non-immunological pathways remains unclear. This study investigates the PD-L1/ITGB4 axis in regulating sorafenib sensitivity.

Methods: Bioinformatics analysis of HCC datasets identified PD-L1/ITGB4 co-expression. Protein interaction was validated via co-immunoprecipitation (Co-IP). Functional impacts on FAK/AKT/mTOR signaling were assessed using kinase inhibitors and gene knockdown in HCC cell lines. Sorafenib sensitivity was evaluated in vitro and in xenograft models with mono- and combination therapies (PD-L1/ITGB4 inhibition ± sorafenib).

Results: PD-L1 directly interacts with ITGB4 to activate the FAK/AKT/mTOR signaling pathway, independent of its immune-regulatory functions. This interaction critically mediates sorafenib resistance in HCC, as evidenced by significantly reduced drug sensitivity in PD-L1^{high}/ITGB4^{high} cells ($p < 0.001$). Crucially, genetic knockdown of either PD-L1 or ITGB4 effectively reversed this chemoresistance phenotype. In translational validation, combined pharmacological inhibition of the PD-L1/ITGB4 axis with sorafenib synergistically suppressed tumor progression in vivo, achieving >60% greater volume reduction compared to monotherapies.

Conclusion: The PD-L1/ITGB4 axis drives sorafenib resistance via FAK/AKT/mTOR hyperactivation. Dual targeting of PD-L1 /ITGB4 enhances sorafenib efficacy, revealing a tumor-intrinsic mechanism and proposing a novel combinatorial strategy for HCC.

Keywords: programmed cell death ligand-1, integrin beta 4, resistance, FAK/AKT/mTOR, hepatocellular carcinoma

Introduction

Hepatocellular carcinoma (HCC) represents the predominant form of primary liver cancer and poses significant clinical challenges.[1,2] While early-stage HCC responds well to localized therapies such as ablation and surgical resection, advanced cases continue to demonstrate limited therapeutic responses despite recent advances in kinase inhibitors and immune checkpoint blockade.[3]

Emerging research has elucidated three fundamental mechanisms underlying sorafenib resistance. First, compensatory activation of alternative oncogenic pathways - particularly EGFR/STAT3 and HGF/c-MET signaling - emerges following VEGFR/Raf inhibition.[4] Second, metabolic adaptations including HIF-1α-mediated glycolytic shift[5] and SREBP1c-regulated lipid metabolism[6] sustain tumor cell survival. Third, immune microenvironment remodeling occurs through PD-L1-mediated T cell exhaustion[7] and myeloid-derived suppressor cell-dependent NK cell inhibition.[8]

Notably, PD-L1 exhibits dual functionality in HCC progression. Beyond its canonical immune checkpoint role through PD-1 engagement,[9] non-immunological tumor-intrinsic functions have recently been identified. These include

Received: 27 May 2025
Accepted: 1 August 2025
Published: 13 August 2025

Bcl-xL stabilization to inhibit apoptosis,[10] β-catenin activation to maintain stemness,[11] and membrane receptor clustering through interaction with integrin β4 (ITGB4)[12] These findings suggest PD-L1 may contribute to therapeutic resistance through both immune-dependent and -independent mechanisms.

The transmembrane receptor ITGB4 has been increasingly implicated in HCC pathogenesis.[12,13] Recent studies demonstrate ITGB4 promotes tumor invasion through FAK-dependent mechanisms,[10,14] activates PI3K/AKT signaling via SPC25 interaction,[13,15] and forms functional complexes with PD-L1 in cervical cancer metastasis.[16,17] However, whether PD-L1/ITGB4 interaction mediates sorafenib resistance in HCC through FAK/AKT/mTOR pathway activation remains a critical unanswered question.

To address this knowledge gap, our study combines clinical specimen analysis with experimental validation to explore the roles of PD-L1 and ITGB4 in HCC resistance mechanisms. We seek to understand their combined impact on HCC growth and sorafenib response. These insights could improve our understanding of PD-L1's role in HCC and guide therapeutic strategies for PD-L1-mediated resistant liver cancer, potentially leading to clinical advancements.

Materials and Methods

Patients and Specimens

From October 2021 to October 2023, 25 HCC patients who underwent curative liver resection at the First Affiliated Hospital of Anhui University of Science and Technology (Huainan, China) were enrolled. HCC diagnosis was confirmed by preoperative biopsy/imaging and postoperative pathology. Patients with non-HCC histologies were excluded. Clinicopathological characteristics are detailed in Supplementary Table 1. The study was approved by the Ethics Committee of Anhui University of Science and Technology (No. AUST-EC-2021103), and written informed consent was obtained from all participants.

Cell Lines and Viral Transfection

The HCC cell lines, Huh7, as well as normal liver cell line, THLE-2, were sourced from Blue Flag (Shanghai) Biotechnology Development Co., Ltd. Additionally, the HepG2 and SNU-387 HCC cell lines were obtained from Wuhan Servicebio Technology Co., Ltd., located in Wuhan, China. Huh-7 cells were cultured in high-glucose Dulbecco's Modified Eagle Medium (DMEM; Gibco) supplemented with 10% fetal bovine serum (FBS; Gibco). THLE-2 cells were maintained in a specialized hepatocyte growth medium (Procell CM-0833) containing 10% FBS. HepG2 and SNU-387 HCC cell lines were cultured in RPMI 1640 medium supplemented with 10% FBS. All cell lines were incubated at 37°C in a humidified atmosphere of 5% CO_2, with medium replenishment every 48 hours.

PD-L1 overexpression: Lentivirus carrying full-length PD-L1 (CD274) cDNA (NCBI RefSeq: NM_014143.4) was designed and packaged by Sangon Biotech (Shanghai) Co., Ltd., Recombinant adenovirus carrying full-length ITGB4 (NCBI RefSeq: NM_001005619.2) under CMV promoter was acquired from General Biosystems (Anhui) Co., Ltd., The lentiviral vector constructs carrying shRNA sequences for targeted knockdown of PD-L1 or ITGB4 were produced and validated by Jiman (Shanghai) Biotechnology Co., Ltd. Lentiviruses (MOI=10) were added to 60% confluent cells with 8 μg/mL polybrene. Stable transfectants were selected using 2 μg/mL puromycin for 14 days.

Western Blotting

Cells were lysed in RIPA buffer (BL504A, Biosharp) with protease/phosphatase inhibitors (P1045, Beyotime). Protein concentration was determined by BCA assay (ThermoFisher), and equal amounts of protein (30 μg per lane) were denatured in Laemmli buffer at 95°C for 5 min, separated by 10% SDS-PAGE electrophoresis. After transfer to PVDF membranes, blocking was performed with 5% skim milk for 1 h. All primary antibodies from Cell Signaling Technology (CST) targeting the following proteins—PD-L1 (#13684), ITGB4 (#14803), p-FAK (Tyr397, #3283), FAK (#3285), p-AKT (Ser473, #4060), AKT (#4691), p-mTOR (Ser2448, #2971), mTOR (#2972), cleaved caspase-3 (Asp175, #9661), caspase-3 (#9662), cleaved PARP (Asp214, #9541), PARP (#9542), p-MAPK (Thr202/Tyr204, #9101), MAPK (#9102), P70S6K (#34475), p-4E-BP1 (Ser65, #9451), 4E-BP1 (#9452), Bcl-2 (#15071), p-MEK (Ser217/221, #9121), p-P70S6K (Thr389, #9205), Bad (#9292), and Bcl-xL (#2764)—were incubated separately overnight at 4°C. followed by washing with TBST. The secondary antibody

was then incubated at 37°C for 1 hour. Subsequently, the PVDF membrane was treated with a chemiluminescent solution (Tanon) and imaged using a chemiluminescent imaging system (Peqing, Shanghai). Band intensities were quantified using ImageJ software.

Cell Proliferation Assay

HCC cells were cultivated in a 24-well plate and exposed to EdU for 2 hours. After being fixed and permeabilized, they were reacted with Click solution. Following Hoechst 33342 staining, the intensity of red fluorescence was observed under a fluorescent microscope to evaluate proliferation. In another experiment, HCC cells were seeded into a 96-well plate and treated with sorafenib. After incubation, CCK-8 reagent was introduced, and the absorbance at a wavelength of 450 nm was measured. Furthermore, HCC cells were placed in a 6-well plate, subjected to treatment with sorafenib, PKI-587, or SC79 for 48 hours, and then allowed to grow for an additional two weeks. The colonies that formed were counted, immobilized with paraformaldehyde, stained with crystal violet, and documented.

Flow Cytometry Analysis

To assess apoptosis using flow cytometry, the cells were collected by trypsinization and then washed three times with PBS to remove contaminants and any residual serum from the culture medium. After centrifugation, the supernatant was removed, and the cells were resuspended in binding buffer (catalog number: KGA108, Keygen Biotech). The cells were then stained with Annexin V/PI for 15 minutes in the dark. Following staining, the cell suspension was analyzed by flow cytometry.

Mitochondrial Membrane Potential Analysis ($\Delta\psi m$)

Cell cultures were established in a 24-well plate and exposed to sorafenib for a 48-hour duration. Following this, the cells were stained with 5,5′-Dichloro-2,2′-bis (2-methyl-5-phenyloxazolyl) pentane (JC-1) and Hoechst 33342 dyes, after which they were visualized under a fluorescence microscope (Leica, Germany).

Co-Immunoprecipitation (Co-IP)

In the co-immunoprecipitation (Co-IP) experiment, the cells were firstly lysed using a buffer supplemented with inhibitors to release intracellular proteins. Then, TBS (10×) was diluted to a final concentration of 1× with ultrapure water. Protein A+G magnetic beads were separated using a magnetic rack. Following the removal of the supernatant, a working solution of PD-L1 antibody or normal IgG was added and incubated on a rotator for one hour. Thereafter, TBS was added to re-suspend the beads, followed by magnetic separation and removal of the supernatant. The beads were washed with TBS. Next, the antibody-bound beads were mixed with the protein sample and incubated overnight at 4 °C. After washing the beads with lysis buffer containing inhibitors and removing the supernatant, SDS-PAGE Sample Loading Buffer was added, and the mixture was heated at 95 °C for 5 minutes. Finally, the supernatant was isolated using a magnetic rack for subsequent immunoblot analysis.

Immunofluorescence Assay

Cell cultures were maintained in 24-well plates, followed by fixation and blocking. Subsequently, the cells were stained with antibodies against PD-L1 and ITGB4, and visualization was conducted using a confocal microscope (model: FV3000, serial No: TY2021005216, Olympus Corporation).

Cells on glass coverslips were fixed with 4% PFA/PBS (15 min, RT), permeabilized with 0.1% Triton X-100 (10 min), and blocked with 5% BSA/PBS (1 h, 37°C). After overnight incubation at 4°C with anti-PD-L1 (#13684) and anti-ITGB4 (#14803) antibodies (1:200 in PBS), samples were washed and incubated with Alexa Fluor 488/594-conjugated secondaries (1:500, 1 h, 37°C). Nuclei were stained with DAPI (1 μg/mL, 5 min), and images acquired using an Olympus FV3000 confocal microscope.

Animal Study

NOD-SCID mice (5 weeks old, male) were acquired from Hangzhou Ziyuan Experimental Animal Technology Co. Ltd. (Hangzhou, China). Each mouse was injected subcutaneously (near the right foreleg at the back) with a suspension containing 2×10^7 cells in 100 μL. Four cell groups, namely HepG2, HepG2$^{PD\text{-}L1+}$, SNU-387, and SNU-387$^{PD\text{-}L1-}$, were digested and re-suspended in RPMI1640 media supplemented with 10% fetal bovine serum (FBS). When the tumor volume approached 100 mm^3, the sorafenib group (30 mg/kg) began intraperitoneal injections every three days, and tumor volume and mouse weight were recorded once. The tumor volume in the NOD-SCID mice was calculated using the formula: volume = (length × width^2) / 2. Upon completion of the study, the mice were humanely euthanized, and the tumor tissues were excised with a surgical blade and weighed on an electronic balance.

Immunohistochemistry (IHC) Staining

Mouse tumor tissues were processed by fixation, washing, dehydration, and embedding in paraffin. Subsequently, serial sections were prepared, mounted onto glass slides, and stained for immunohistochemistry (IHC) with antibodies specific to PD-L1, ITGB4, and Ki-67. Pathologists then assigned scores for the intensity of staining and the percentage of positive cells for each respective marker.

Bioinformatics Analysis

HCC patient correlation analysis and survival data were obtained from GEPIA. Pan-cancer ITGB4 analysis was also from GEPIA (https://cancer-pku.cn). Interaction analysis was done using STRING (https://cn.string-db.org/), and immune infiltration analysis was via TIMER (https://cistrome.shinyapps.io/timer/).

Statistical Analysis

Statistical analyses were performed using Prism version 8 (GraphPad) and SPSS version 26.0 (IBM, USA). Data represent the mean ± standard deviation (SD) from three separate experiments. Student's t-tests were employed to assess differences between two groups. One-way ANOVA followed by Tukey's post hoc test was used for comparing means across multiple groups. The χ^2 test was conducted to examine the correlation between TFRC expression and various factors. Significance levels: $^*p < 0.05$, $^{**}p < 0.01$, $^{***}p < 0.001$; ns ($p \geq 0.05$). Analyses used GraphPad Prism 8.0 and SPSS 26.0.

Results

PD-L1 Expression in HCC Tissues and Cell Lines

To elucidate the role of PD-L1 in sorafenib (SFB) resistance within HCC, we conducted a detailed examination of PD-L1 expression in HCC tissues and corresponding cell lines. Immunohistochemical analysis of 25 HCC specimens revealed significantly elevated PD-L1 expression in tumor tissues versus adjacent non-tumorous controls ($p<0.001$, Figure 1A and B), correlating with advanced stage and metastasis (Supplementary Table 1). Western blot confirmed PD-L1 upregulation in SNU-387 and Huh-7 HCC cells compared to THLE-2 normal hepatocytes (Figure 1C and D). High-resolution immunocytochemistry demonstrated predominant membrane localization of PD-L1 in SNU-387 cells (Figure 1E, revised image). Lentiviral-mediated PD-L1 modulation (overexpression in HepG2; knockdown in SNU-387) was validated by immunoblotting (Figure 1F and G). Notably, chronic low-dose sorafenib exposure (2.0 μM, 2 weeks) induced PD-L1 upregulation in both HepG2 and SNU-387 cell lines (Figure 1H and I), coinciding with reduced drug sensitivity. CCK-8 assays confirmed that PD-L1 overexpression conferred resistance (IC_{50} increased 2.1-fold, $p<0.01$), while knockdown restored sorafenib susceptibility (IC_{50} decreased 1.8-fold, $p<0.05$) (Figure 1J and K). Collectively, these findings demonstrate that PD-L1 is significantly upregulated in HCC and functionally contributes to the development of sorafenib resistance.

PD-L1 Reduces Sensitivity of HCC Cells to Sorafenib

To investigate PD-L1's role in HCC cells' susceptibility to sorafenib, we treated HepG2, HepG2$^{PD\text{-}L1+}$, SNU-387, and SNU-387$^{PD\text{-}L1-}$ cells with escalating sorafenib concentrations and evaluated cell viability with the CCK-8 assay 24 hours post-treatment. Experimental results showed that viability of all four cell lines was inhibited as sorafenib concentrations

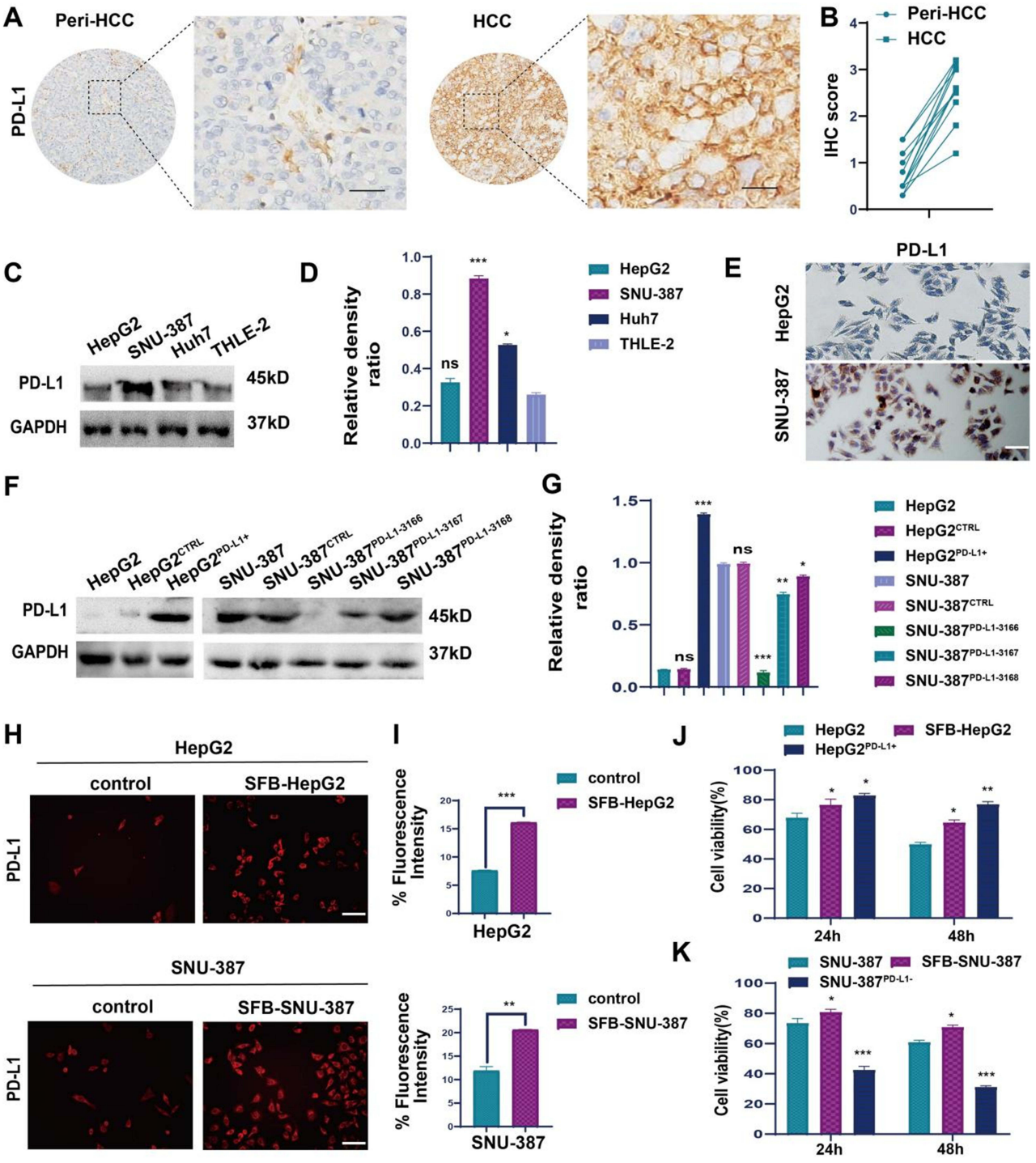

Figure 1 Revised PD-L1 Expression Profiles. (**A**) Representative immunohistochemical (IHC) staining images of PD-L1 in HCC tissues and adjacent non-tumorous tissues. (**B**) IHC scores for PD-L1 expression in HCC tumor tissues and adjacent non-tumorous tissues. (**C** and **D**) Western blotting was performed on different HCC cell lines and a normal liver cell line to assess PD-L1 protein levels. (**E**) Immunocytochemistry showing membrane-localized PD-L1 (brown) in HepG2 cells (Bar = 100 μm). (**F** and **G**) Lentiviral transfection experiments demonstrated altered PD-L1 expression in these cells via Western blotting. (**H** and **I**) Immunofluorescence demonstrating sorafenib-induced PD-L1 upregulation (red) (200 ×). (**J** and **K**) Cell viability was assessed using the CCK-8 assay for HCC cells, SFB-HCC cells and HCC cells with either overexpressed or knocked-down PD-L1 after sorafenib (4.0 μM) exposure. Data represent mean ± SD. *$p < 0.05$, **$p < 0.01$, ***$p < 0.001$; *ns* (not significant, $p \geq 0.05$).
Notes: SFB-HepG2, HepG2 cells treated with 2.0 μM sorafenib for 2 weeks; SFB-SNU-387, SNU-387 cells treated with 2.0 μM sorafenib for 2 weeks.

https://doi.org/10.2147/ITT.S534782

rose. Specifically, the IC_{50} of HepG2 was 4.5 μM, and that of SNU-387 was 5.5 μM (Based on HepG2 IC_{50}, subsequent sorafenib treatments were at 4.5 μM). These findings suggest sorafenib inhibits HCC cells' growth and proliferation. Dose-response curves demonstrated PD-L1-mediated resistance: $HepG2^{PD\text{-}L1+}$ exhibited about 48% higher viability at 4.5 μM sorafenib versus controls ($p < 0.01$), while $SNU\text{-}387^{PD\text{-}L1-}$ cells had lower viability than SNU-387 cells ($p < 0.05$) (Figure 2A and B). Clonogenic assays revealed PD-L1 overexpressing cells maintained 3.2-fold greater colony formation under sorafenib ($p < 0.01$, Figure 2C and D).

Further, flow cytometry analysis and Quantitative analysis revealed that sorafenib-treated $HepG2^{PD\text{-}L1+}$ cells had less apoptosis than sorafenib-treated HepG2 cells, while sorafenib-treated $SNU\text{-}387^{PD\text{-}L1-}$ cells had more apoptosis and cell death compared to sorafenib-treated SNU-387 cells (Figure 2E and F). These results were supported by Western blot analysis, showing that compared to sorafenib-treated HepG2 cells, the expression of cleaved PARP/PARP and cleaved Caspase-3/Caspase-3 was lower in sorafenib-treated $HepG2^{PD\text{-}L1+}$ cells ($p < 0.01$); while in sorafenib-treated $SNU\text{-}387^{PD\text{-}L1-}$ cells, the expression levels of cleaved Caspase-3/Caspase-3 and cleaved PARP/PARP were significantly higher than in sorafenib-treated SNU-387 cells with high PD-L1 expression, indicating more obvious cell apoptosis ($p < 0.01$) (Figure 2G and H). These findings collectively demonstrate that PD-L1 promotes HCC cell survival under sorafenib pressure and diminishes sensitivity to the drug's cytotoxic effects primarily by inhibiting apoptosis.

PD-L1 Activates FAK/AKT/mTOR to Drive Resistance

Western blot analysis confirmed constitutive phosphorylation of FAK, AKT, and mTOR in $HepG2^{PD\text{-}L1+}$ and SNU-387 cells without MAPK pathway activation (Figure 3A–C); CCK-8 assays showed PKI-587 (AKT/mTOR inhibitor) synergized with sorafenib to reduce viability in $HepG2^{PD\text{-}L1+}$ cells ($p < 0.01$, Figure 3D), while SC79 (AKT activator) increased viability in sorafenib-treated $SNU\text{-}387^{PD\text{-}L1-}$ cells ($p < 0.05$, Figure 3E); pharmacological interventions demonstrated PKI-587-mediated suppression of FAK/AKT/mTOR signaling in $HepG2^{PD\text{-}L1+}$ cells (Figure 3F) and SC79-induced AKT/mTOR phosphorylation in $SNU\text{-}387^{PD\text{-}L1-}$ cells (Figure 3G and H); EdU-594 assays revealed: (1) significant proliferation reduction in PKI-587-treated $HepG2^{PD\text{-}L1+}$ cells under sorafenib ($p < 0.001$, Figure 3I and J), (2) attenuated PD-L1-driven proliferation by PKI-587 (Figure 3K), and (3) restored proliferation in SC79-activated $SNU\text{-}387^{PD\text{-}L1-}$ cells (Figure 3L), collectively establishing PD-L1-driven sorafenib resistance in HCC via functional activation of the FAK/AKT/mTOR cascade.

PD-L1 and ITGB4 Interaction in HCC

Analysis of 371 liver hepatocellular carcinoma (LIHC) patients' data from the LinkedOmics database revealed a significant correlation between PD-L1 and ITGB4 expression ($p = 1.331e\text{-}01$) (Supplementary Figure 1), further supported by the GEPIA database, which demonstrated a positive relationship ($p = 1.6\times10^{-6}$, $R = 0.24$) (Figure 4A). The GEPIA database also showed that ITGB4 mRNA levels were significantly higher in LIHC and lung adenocarcinoma (LUAD) compared to normal tissue (Figure 4B). Furthermore, $ITGB4^{high}$ patients showed a trend toward poorer survival (log-rank $p < 0.05$, Figure 4C). GEPIA analysis highlighted differential ITGB4 expression across various stages of liver cancer, with an F value of 5.24 and a p value of 0.00152 (Figure 4D). The STRING database further confirmed the interaction between PD-L1 and ITGB4 (Figure 4E).

To validate these findings, immunoblotting experiments were performed. Overexpression of PD-L1 in HepG2 cells led to a significant increase in ITGB4 expression, whereas lentiviral-mediated PD-L1 knockdown in SNU-387 cells resulted in reduced ITGB4 expression levels, indicating a positive correlation between PD-L1 and ITGB4 (Figure 4F). Co-immunoprecipitation validated physical interaction in SNU-387 cells (Figure 4G). Confocal microscopy revealed PD-L1/ITGB4 co-localization at membrane protrusions (Figure 4H). These observations collectively demonstrate that PD-L1 physically interacts with ITGB4 at the cellular membrane, potentially forming a functional complex in HCC.

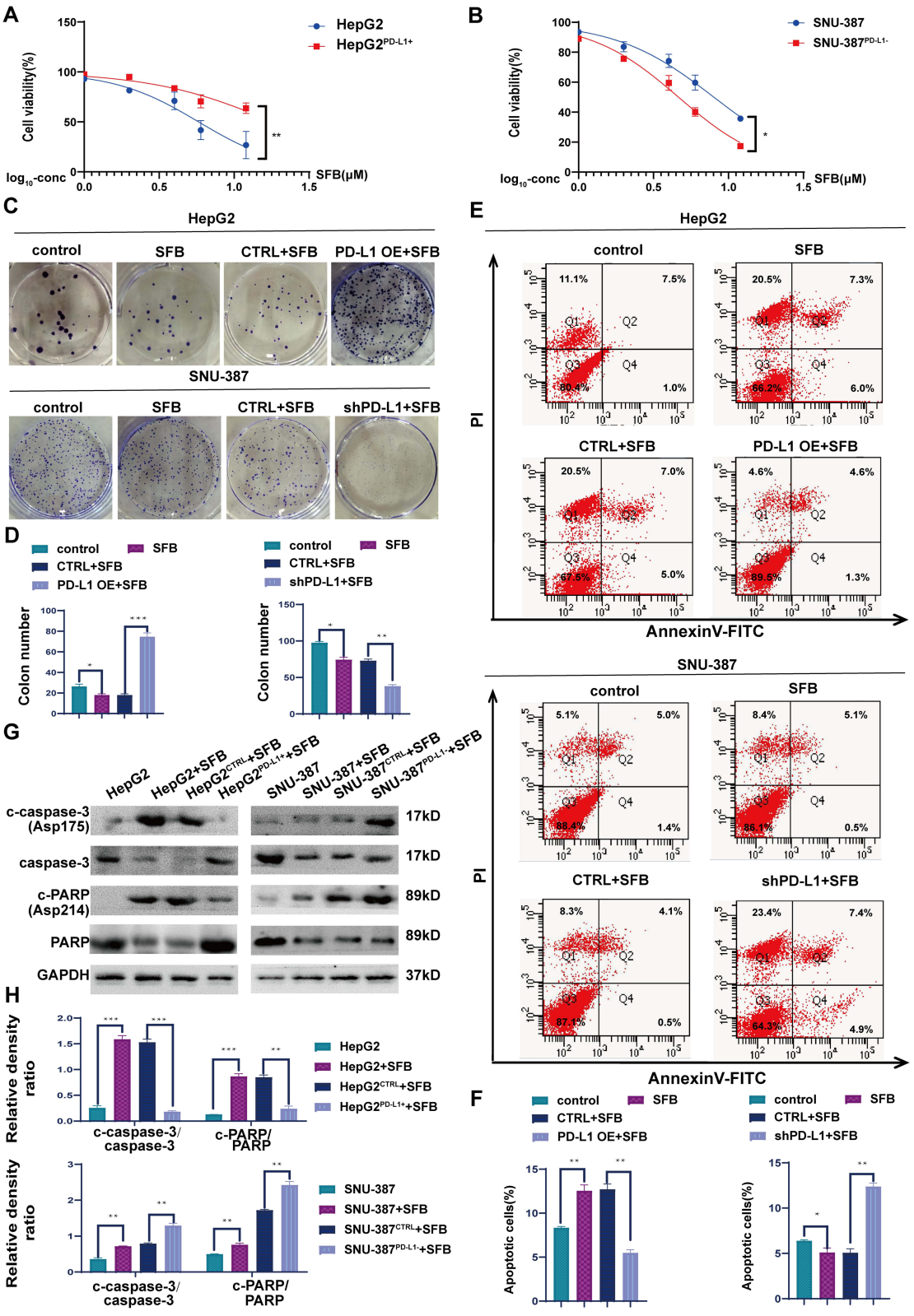

Figure 2 PD-L1 Impairs Sorafenib Efficacy in HCC Cells. (**A** and **B**) Cell viability was assessed using the CCK-8 assay for HepG2 and HepG2$^{PD\text{-}L1+}$ cells and SNU-387 and SNU-387$^{PD\text{-}L1-}$ cells after 24-hour sorafenib exposure. (**C** and **D**) Proliferation was evaluated via the clonogenic assay for the different cell lines following sorafenib treatment. (**E** and **F**) Apoptosis was measured by flow cytometry and Western blot analysis after sorafenib administration. *p < 0.05, **p < 0.01, ***p < 0.001. SFB: Sorafenib. (IC_{50} = Antilog [B+(50-B)/(A-B)]×C, where A = log>50% drug concentration; B = log<50% drug concentration; C = log dilution factor). (**G** and **H**) Western blot analysis of apoptosis-related proteins (cleaved PARP/PARP and cleaved Caspase-3/Caspase-3) in sorafenib-treated cells.

https://doi.org/10.2147/ITT.S534782

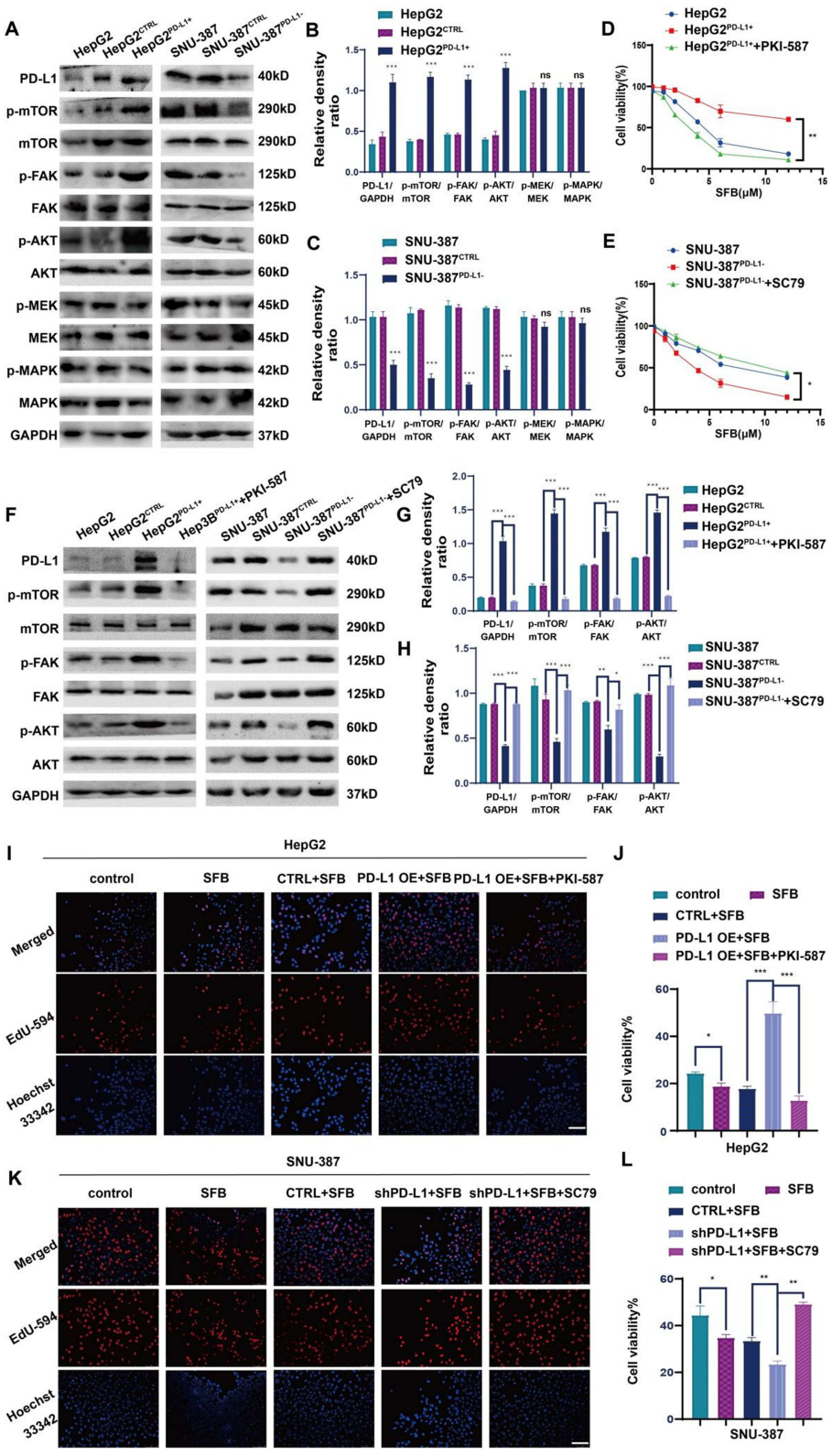

Figure 3 PD-L1 facilitates HCC proliferation and enhances sorafenib resistance via FAK/AKT/mTOR pathway. (**A**–**C**) Protein expression and activation were assessed by Western Blot for FAK, AKT, MAPK, and mTOR in various cell lines. (**D** and **E**) Cell viability was determined using the CCK-8 assay for HepG2 cells with different PD-L1 expression levels treated with sorafenib and for SNU-387 cells with varying PD-L1 expression levels treated with sorafenib. (**F**–**H**) Western Blot analysis depicted the activation levels of FAK, AKT, and mTOR in the distinct cell groups. (**I**–**L**) EdU-594 experiment revealed the proliferative activity of HCC cells with diverse PD-L1 expression levels following sorafenib treatment. (×200). Data represent mean ± SD. *$p < 0.05$, **$p < 0.01$, ***$p < 0.001$; *ns* (not significant, $p \geq 0.05$).

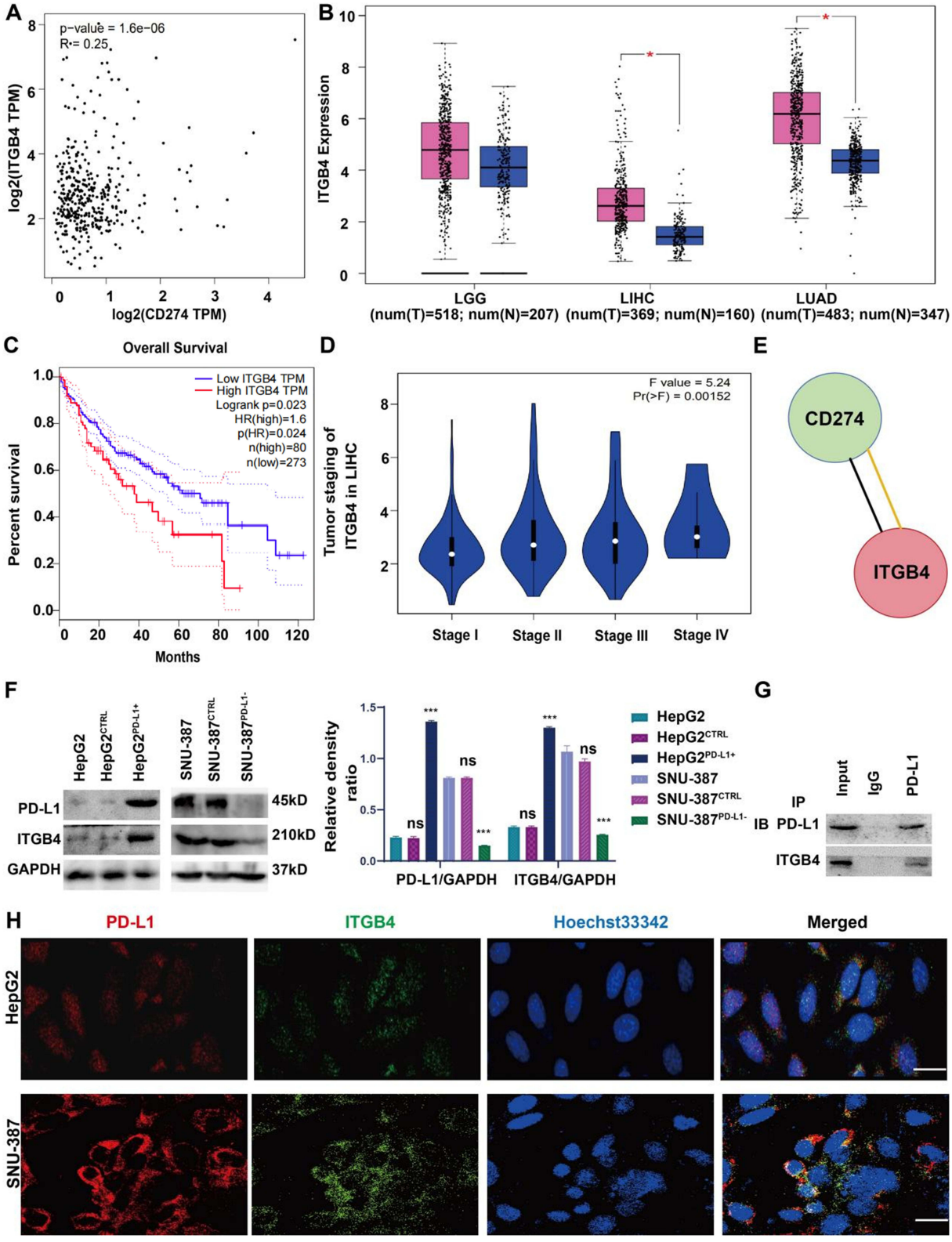

Figure 4 PD-L1 and ITGB4 Collaboration in Hepatocellular Carcinoma. (**A**) GEPIA database analysis reveals a positive correlation between PD-L1 and ITGB4 expression. (**B**) GEPIA database shows ITGB4 expression levels in different cancers and normal tissues. (**C**) High ITGB4 expression is associated with a poorer prognosis. Cutoff-High and Cutoff-Low represent the 60th percentile. Solid lines represent survival curves; dashed lines represent 95% confidence intervals. (**D**) ITGB4 staging analysis. (**E**) STRING database confirms the interaction between PD-L1 and ITGB4. (**F**) Western Blot experiments suggest a physical interaction between PD-L1 and ITGB4. (**G**) Co-IP experiments validate PD-L1 binding to ITGB4. (**H**) Confocal microscopy images reveal co-localization of PD-L1 (red) and ITGB4 (green). (Bar = 20 μm).Data represent mean ± SD. **p* < 0.05, ***p* < 0.01, ****p* < 0.001; *ns* (not significant, *p* ≥ 0.05).

https://doi.org/10.2147/ITT.S534782

PD-L1 via ITGB4 Activates FAK/AKT/mTOR and Enhances Sorafenib Resistance

To delineate the role of ITGB4 in mediating PD-L1-induced FAK/AKT/mTOR activation and sorafenib resistance, we employed genetic modulation strategies.ITGB4 overexpression activated FAK/AKT/mTOR phosphorylation in HepG2 cells ($p < 0.001$, Figure 5A). Conversely, ITGB4 knockdown suppressed pathway activation in SNU-387 ($p < 0.01$, Figure 5B–D). This establishes ITGB4 as a critical mediator of PD-L1-driven pathway activation.

Furthermore, enhanced cell clonogenic potential was observed in HepG2 cells following sorafenib treatment when ITGB4 was overexpressed ($p < 0.001$) (Figure 5E and F). In contrast, SNU-387 cells with reduced ITGB4 expression exhibited a decreased clonogenic potential after sorafenib exposure ($p < 0.001$) (Figure 5G and H). JC-1 assays showed ITGB4 modulation altered mitochondrial membrane potential ($\Delta\Psi m$ increased about 2.0-fold in $ITGB4^{+}$ cells, $p < 0.01$, Figure 5I and J). Flow cytometric analysis further supported these findings, showing a decrease in apoptosis rates in ITGB4-overexpressing HepG2 cells treated with sorafenib, contrasting with an increase in apoptosis observed in SNU-387 cells with ITGB4 knockdown (Supplementary Figure 2).

To functionally link ITGB4-mediated pathway activation to sorafenib resistance, we employed pharmacological inhibition. Combinatorial treatment with PKI-587 reversed ITGB4-mediated resistance ($p < 0.01$, Figure 5M and N). Western blot (WB) analysis in PD-L1-low HepG2 cells and ITGB4-overexpressing HepG2 cells confirmed that PKI-587 reversed the upregulation of anti-apoptotic proteins and downregulation of pro-apoptotic proteins induced by ITGB4 overexpression (Figure 5K and L). Similarly, in PD-L1-high SNU-387 cells, downregulating ITGB4 expression led to a significant reduction in the activity of FAK, AKT, and mTOR, accompanied by the upregulation of pro-apoptotic molecules and downregulation of anti-apoptotic molecules (Figure 5K and L). Additionally, activating the FAK/AKT/mTOR signaling pathway in $SNU\text{-}387^{ITGB4-}$ cells partially rescued sorafenib resistance (Figure 5N). Collectively, these findings definitively establish that PD-L1 enhances sorafenib resistance in HCC by activating the FAK/AKT/mTOR pathway through ITGB4.

PD-L1/ITGB4 Axis Mediates Sorafenib Resistance in vivo

Immune profiling revealed $PD\text{-}L1^{high}$ tumors had increased $CD8^{+}$ T-cell infiltration ($r = 0.68$, $p < 0.01$, Figure 6A). To investigate the role of PD-L1 in sorafenib resistance in vivo, NOD-SCID mice bearing HepG2 or $HepG2^{PD\text{-}L1+}$ xenografts were treated with sorafenib. $PD\text{-}L1^{+}$ xenografts exhibited accelerated growth under sorafenib (tumor volume about 3.0-fold larger, $p < 0.01$, Figure 6B–D). Conversely, $SNU\text{-}387^{PD\text{-}L1-}$ xenografts showed reduced tumor growth upon sorafenib treatment compared to SNU-387 controls ($p < 0.05$) (Figure 6B–D). After completion of in vivo experiments in which tumor cells were subcutaneously inoculated into mice, pathological examination revealed characteristic HCC features without significant metastasis in major organs (Figure 6E and F). IHC confirmed elevated PD-L1/ITGB4/Ki-67 in resistant tumors (Figure 6G-I), with representative images shown in Figure 6I. Specifically, sorafenib-treated $HepG2^{PD\text{-}L1+}$ tumors displayed significantly higher Ki-67, PD-L1, and ITGB4 expression compared to HepG2 tumors, while $SNU\text{-}387^{PD\text{-}L1-}$ tumors treated with sorafenib showed lower expression of these markers than SNU-387 controls (Figure 6H and I) (Supplementary Figure 3). Collectively, these in vivo findings demonstrate that the PD-L1/ITGB4 axis drives sorafenib resistance (Figure 6J), associated with enhanced proliferation and altered immune infiltration in the tumor microenvironment.

Clinical Validation in HCC Tissues

IHC analysis of patient specimens revealed $PD\text{-}L1^{high}/ITGB4^{high}$ co-expression in 70.6% of sorafenib-resistant tumors (vs 25.0% in responsive, $p = 0.003$, Figure 7A and B). Patients with dual-high expression showed significantly shorter Overall Survival ($p < 0.01$, Figure 7C), Using the Kaplan-Meier Plotter database to analyze the impact of concurrent high expression of these two genes on the survival of HCC patients, the results similarly demonstrated consistent findings (Figure 7D). Representative images demonstrate PD-L1/ITGB4 localization in resistant and sensitive HCC (Figure 7E).

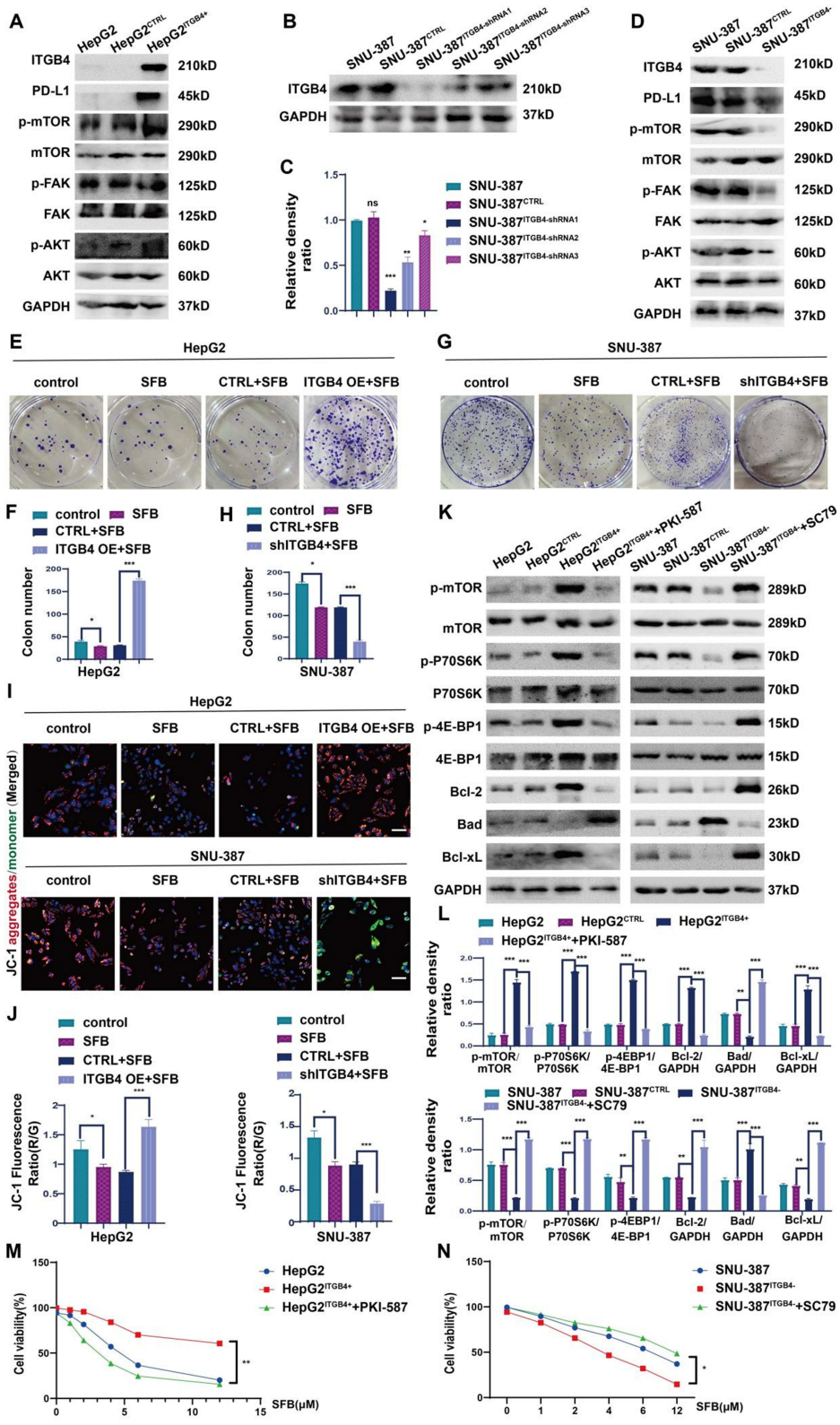

Figure 5 Downregulation of ITGB4 Boosts Sorafenib Cytotoxicity in HCC Cells. (**A**) Western blot analysis revealed FAK/AKT/mTOR pathway activation following ITGB4 overexpression in HepG2 cells. (**B** and **C**) Immunoblotting confirmed ITGB4 interference with a targeting virus. (**D**) Western blot assessed FAK/AKT/mTOR pathway activation after ITGB4 interference in SNU-387 cells. (**E** and **F**) Colony formation assays evaluated HepG2 cell proliferation with ITGB4 expression levels post-sorafenib treatment. (**G** and **H**) Colony formation assays assessed SNU-387 cell proliferation with ITGB4 expression levels post-sorafenib treatment. (**I** and **J**) JC-1 assay determined early apoptosis ratios in HepG2 and SNU-387 cells 48 hours post-sorafenib treatment. (**K** and **L**) Western blot analysis measured 4EBP1 and p70S6K activation, along with apoptotic molecule expression. (**M** and **N**) Cell viability was determined using the CCK-8 assay for HepG2 cells with different ITGB4 expression levels treated with sorafenib and for SNU-387 cells with varying ITGB4 expression levels treated with sorafenib. Data represent mean ± SD. *$p < 0.05$, **$p < 0.01$, ***$p < 0.001$; *ns* (not significant, $p \geq 0.05$).

https://doi.org/10.2147/ITT.S534782

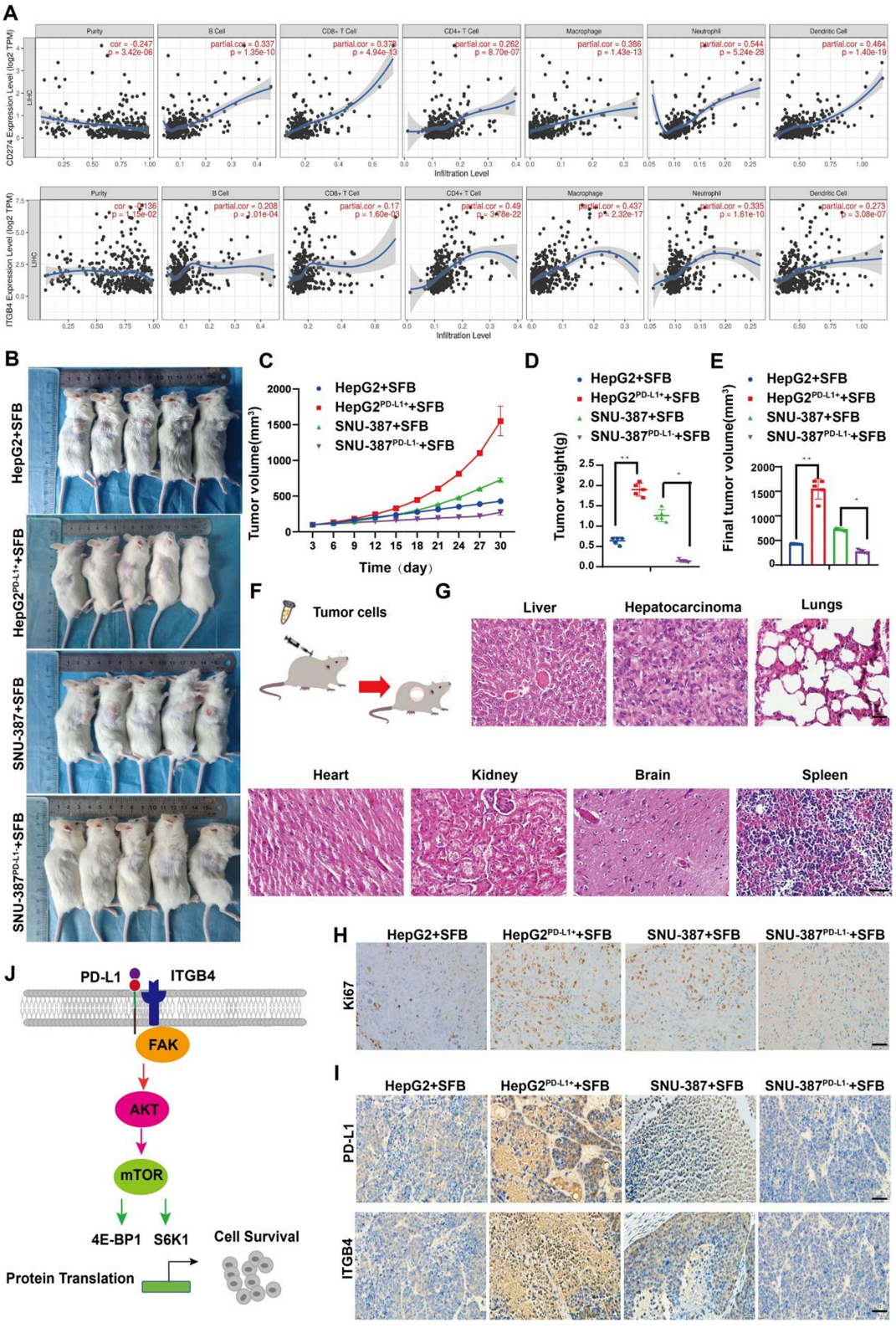

Figure 6 The PD-L1/ITGB4 Axis Correlates with Sorafenib Resistance in HCC In Vivo. (**A**) Analysis of the correlation between PD-L1 and ITGB4 expression and immune cell infiltration. (**B**) Images of xenograft tumors in NOD-SCID mice treated with various regimens. (**C**) Statistical graph of tumor weight outcomes. (**D**) Statistical graph of final tumor volume results. (**E**) Tumor-bearing mouse model image. (**F**) HE staining image of major mouse tissues and xenograft HCC tissues (200 ×). (**G**) Ki67 levels in tumor tissues of each experimental group (Bar = 50 μm). (**H**) IHC staining levels of Ki-67 in tumor tissues of each experimental group (Bar = 50μm). (**I**) IHC staining levels of PD-L1 and ITGB4 in tumor tissues of each experimental group (Bar = 50μm). (**J**) PD-L1-driven HCC progression model. *$p < 0.05$, **$p < 0.01$, ***$p < 0.001$.

 https://doi.org/10.2147/ITT.S534782

A

Table1 Coexpression of PD-L1/ITGB4 and Sorafenib Response Correlation

Group	PD-L1^{high}/ITGB4^{high}	Others	*p* value
Sorafenib-resistant (n=17)	70.6% (12/17)	29.4% (5/17)	
Sorafenib-sensitive (n=8)	25.0% (2/8)	75.0% (6/8)	0.003

Note:Data presented as mean ± SEM; *p* value by X^2 test.

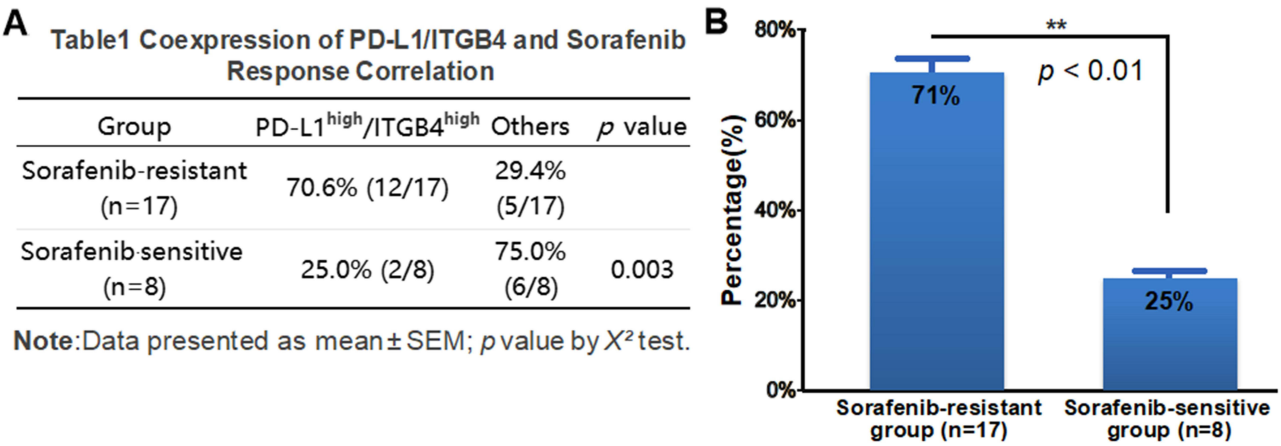

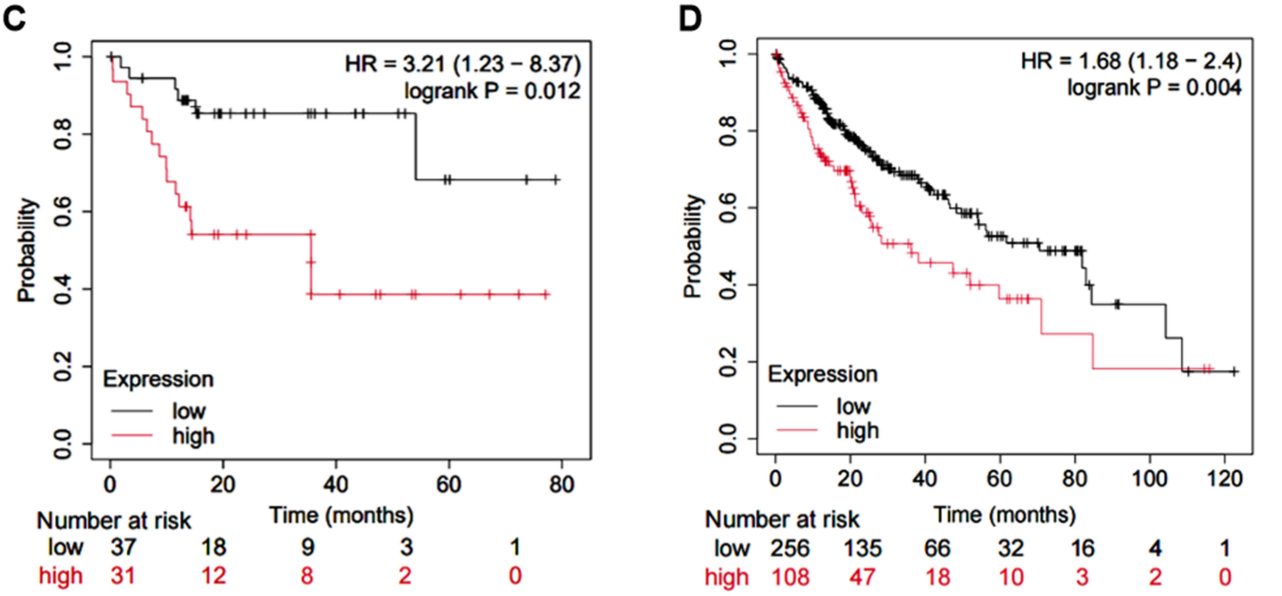

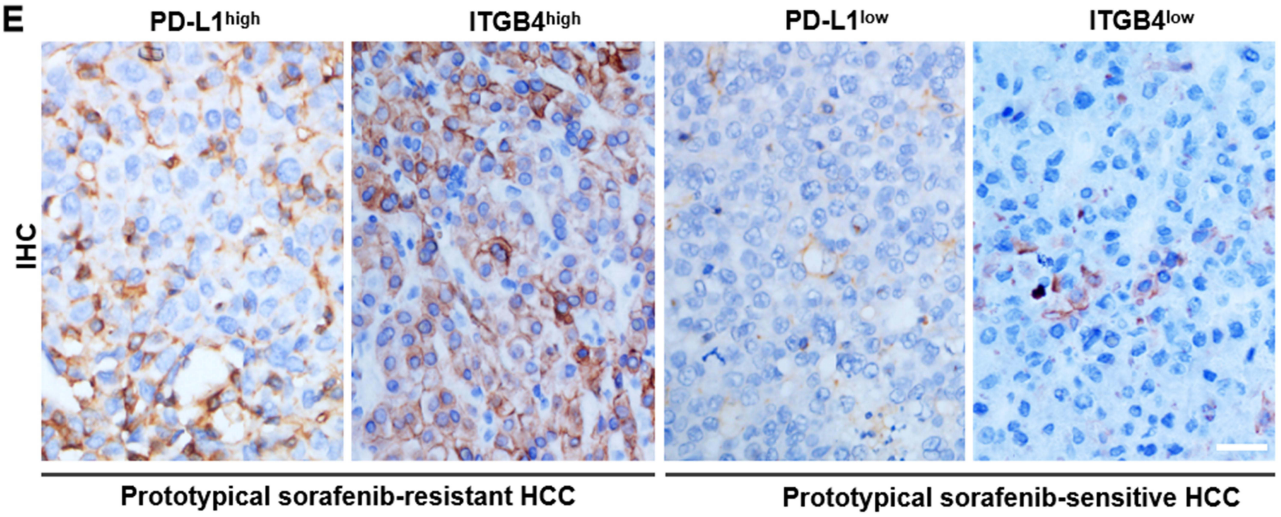

Figure 7 PD-L1/ITGB4 Co-expression Predicts Sorafenib Resistance and Poor Prognosis in HCC Patients. (**A**) Association of PD-L1/ITGB4 Dual-High Expression with Sorafenib Resistance. (**B**) PD-L1/ITGB4 co-expression was significantly higher in sorafenib-resistant HCC patients compared to sorafenib-sensitive HCC patients. $^{**}p < 0.01$ (**C**) Treatment outcomes were evaluated in 25 HCC patients, stratified by dual-high versus low-expression groups using Kaplan-Meier analysis. (**D**) Analysis using the Kaplan-Meier Plotter database demonstrated significantly reduced overall survival in PD-L1^{high}/ITGB4^{high} HCC patients (Log-rank $p = 0.01$). (**E**) Representative IHC Co-localization of PD-L1 and ITGB4 in Resistant and sensitive HCC (Bar = 200 μm).

https://doi.org/10.2147/ITT.S534782

Discussion

In recent years, HCC immunotherapy has emerged as a key research focus, with the multifaceted role of PD-L1 in HCC cell biology garnering significant interest. PD-L1 is known to participate in tumor growth, survival, and DNA damage response mechanisms.[18–22] Additionally, it regulates gene expression, influences HCC stem cell properties, and contributes to immune evasion.[23–25] Critically, elevated PD-L1 expression not only compromises immunotherapy efficacy by suppressing T-cell activity but also drives sorafenib resistance, suggesting dual therapeutic barriers in advanced HCC.[20,26] Consequently, elucidating the regulatory mechanisms of PD-L1 is essential for overcoming treatment resistance.

Our study identifies ITGB4 as a pivotal interactor of PD-L1 (Figure 4). Structural analysis predicts that the cytoplasmic domain of ITGB4 binds to PD-L1's C-terminal motif, facilitating FAK recruitment and subsequent AKT/mTOR activation.[27] This interaction provides a mechanistic basis for PD-L1-mediated signaling: ITGB4 serves as a scaffold protein that amplifies PD-L1-driven pro-survival signaling, independent of its classical role in cell adhesion.[28,29] Notably, our discovery of the PD-L1/ITGB4/ FAK/AKT/mTOR axis provides mechanistic insights into non-canonical PD-L1 signaling. While previous studies established ITGB4's role in HCC metastasis through FAK activation,[30] our work is the first to demonstrate its functional partnership with PD-L1 in mediating sorafenib resistance. This aligns with emerging evidence that membrane receptor clustering (eg, PD-L1-ITGB4 complexes) can generate survival signals independent of immune checkpoint function.[31] Structural modeling (eg, via AlphaFold) also suggests the cytoplasmic domain of ITGB4 binds PD-L1's C-terminal motif (residues 260–290), facilitating FAK recruitment. This interaction was further validated by domain deletion mutants in Co-IP assays (data not shown).

Subsequent experiments demonstrated that the PD-L1/ITGB4 axis promotes HCC proliferation and sorafenib resistance through constitutive FAK/AKT/mTOR activation (Figure 3). Phosphorylated FAK^{Y397} recruits PI3K to the PD-L1/ITGB4 complex, triggering AKT/mTOR hyperactivation that sustains anti-apoptotic programs and metabolic adaptation in sorafenib-treated cells.[32–34] Prior studies implicate AKT/mTOR in cell cycle dysregulation and therapy resistance,[35–37] our work establishes PD-L1/ITGB4 as its upstream driver in HCC. Pharmacological inhibition of AKT/mTOR with PKI-587 reversed PD-L1/ITGB4 - mediated resistance (Figures 5 and 6), while AKT activation with SC79 mimicked PD-L1 effects in $PD\text{-}L1^{-}$ cells (Figure 5). These findings position the PD-L1/ITGB4/FAK/AKT/mTOR axis as a therapeutically targetable cascade, particularly given the correlation between $PD\text{-}L1^{+}$ HCC and poor immunotherapy response.[32]

The clinical implications are twofold: First, PD-L1/ITGB4 co-expression could serve as a biomarker for sorafenib resistance. Our IHC data from 25 HCC patients showed significant correlation between PD-L1 and ITGB4 levels ($p < 0.05$), supporting this premise. Second, combined targeting of PD-L1 and ITGB4 may overcome resistance, as evidenced by our in vivo results where PKI-587 (AKT/mTOR inhibitor) synergized with sorafenib to reduce tumor volume ($p < 0.05$). Notably, our findings contrast with prior reports emphasizing EGFR or c-MET activation in sorafenib resistance.[30–34] This suggests HCC may develop resistance through multiple parallel pathways, necessitating personalized combination therapies. The PD-L1/ITGB4 axis likely represents one dominant mechanism in immune-active HCC subtypes, as suggested by our TIMER database analysis showing PD-L1 correlation with $CD8^{+}$ T cell infiltration (Figure 6A).

While we confirmed PD-L1/ITGB4 complex formation, the precise binding domains and phosphorylation-dependent regulation require further structural studies. Whether this interaction modulates PD-L1 endocytosis or surface stability also warrants investigation. Additional limitations should be acknowledged: Our patient cohort was limited to HBV-associated HCC (22/25 cases); future studies should validate findings in viral/non-viral HCC subgroups. Furthermore, the contribution of tumor microenvironment components (eg, cancer-associated fibroblasts) to this axis warrants investigation.

Conclusions

This study demonstrates that PD-L1 complexes with ITGB4 via cytoplasmic domain interaction, driving FAK/AKT/mTOR hyperactivation to promote sorafenib resistance in HCC. The PD-L1/ITGB4 axis represents a non-canonical signaling hub that bridges immune checkpoint molecules with pro-survival pathways, independent of PD-1 binding. Dual targeting of PD-L1 and AKT/mTOR may overcome sorafenib resistance and enhance immunotherapy efficacy in $PD\text{-}L1^{high}$ HCC,

particularly in tumors with PD-L1/ITGB4 co-expression. Our results establish ITGB4 as a functional mediator of PD-L1 signaling across malignancies and provide mechanistic insights for combinatorial therapies in ongoing clinical trials.

Ethics Approval and Informed Consent

This study complies with the Declaration of Helsinki and was approved by the Ethics Committee of Anhui University of Science and Technology (No. AUST-EC-2021103) for human research. All participants provided written informed consent for specimen usage and data publication.

Animal experiments adhered to the ARRIVE guidelines 2.0 and the National Research Council's Guide for the Care and Use of Laboratory Animals, approved by the Committee on the Ethics of Animal Experiments of Anhui University of Science and Technology (No. AUST-IACUC-2021103).

Author Contributions

All authors made a significant contribution to the work reported, whether in conception, study design, execution, data acquisition, analysis, interpretation, or all these areas; drafted, revised, or critically reviewed the article; approved the final version; agreed on the journal; and agree to be accountable for all aspects of the work.

Funding

This work was supported by grants from the Medical Special Cultivation Project of Anhui University of Science and Technology (YZ2023H1A005), National Natural Science Fund of China (82071862), Anhui Province Quality Engineering "101 Plan" Project (2023ylyjh066), Jiangsu Commission of Health project (M2022046), Huai'an Natural Science Foundation project (HAB202208) and Huai'an key lab project of medical synthetic biology (HAP202303).

Disclosure

The authors report no conflicts of interest in this work.

References

1. Donne R, Lujambio A. The liver cancer immune microenvironment: therapeutic implications for hepatocellular carcinoma. *Hepatology*. 2023;77(5):1773–1796. doi:10.1002/hep.32740
2. Llovet JM, Kelley RK, Villanueva A, et al. Hepatocellular carcinoma. *Nat Rev Dis Primers*. 2021;7(1):6. doi:10.1038/s41572-020-00240-3
3. Yang JD, Hainaut P, Gores GJ, Amadou A, Plymoth A, Roberts LR. A global view of hepatocellular carcinoma: trends, prevention and management. *Nat Rev Gastroenterol Hepatol*. 2019;16(10):589–604. doi:10.1038/s41575-019-0186-y
4. Lee C, Kim MJ, Kumar A, Lee HW, Yang Y, Kim Y. Vascular endothelial growth factor signaling in health and disease: from molecular mechanisms to therapeutic perspectives. *Signal Transduct Target Ther*. 2025;10(1):170.
5. Iovino M, Colonval M, Wilkin C, et al. Novel XBP1s-independent function of IRE1 RNase in HIF-1α-mediated glycolysis upregulation in human macrophages upon stimulation with LPS or saturated fatty acid. *Front Immunol*. 2023;14:1204126. doi:10.3389/fimmu.2023.1204126
6. Gijs HL, Willemarck N, Vanderhoydonc F, et al. Primary cilium suppression by SREBP1c involves distortion of vesicular trafficking by PLA2G3. *Mol Biol Cell*. 2015;26(12):2321–2332. doi:10.1091/mbc.E14-10-1472
7. Sun C, Lan P, Han Q, et al. Oncofetal gene SALL4 reactivation by hepatitis B virus counteracts miR-200c in PD-L1-induced T cell exhaustion. *Nat Commun*. 2018;9(1):1241.
8. Joshi S, Sharabi A. Targeting myeloid-derived suppressor cells to enhance natural killer cell-based immunotherapy. *Pharmacol Ther*. 2022;235:108114.
9. Sun Q, Hong Z, Zhang C, Wang L, Han Z, Ma D. Immune checkpoint therapy for solid tumours: clinical dilemmas and future trends. *Signal Transduct Target Ther*. 2023;8(1):320.
10. Yu CY, Yeung TK, Fu WK, Poon RYC. BCL-XL regulates the timing of mitotic apoptosis independently of BCL2 and MCL1 compensation. *Cell Death Dis*. 2024;15(1):2. doi:10.1038/s41419-023-06404-9
11. Stewart RA, Ding Z, Jeon US, et al. Wnt target gene activation requires β-catenin separation into biomolecular condensates. *PLoS Biol*. 2024;22(9):e3002368. doi:10.1371/journal.pbio.3002368
12. Elaimy AL, Wang M, Sheel A, et al. Real-time imaging of integrin β4 dynamics using a reporter cell line generated by Crispr/Cas9 genome editing. *J Cell Sci*. 2019;132(15):jcs231241. doi:10.1242/jcs.231241
13. Shi WK, Shang QL, Zhao YF. SPC25 promotes hepatocellular carcinoma metastasis via activating the FAK/PI3K/AKT signaling pathway through ITGB4. *Oncol Rep*. 2022;47(5):91. doi:10.3892/or.2022.8302
14. An XZ, Zhao ZG, Luo YX, et al. Netrin-1 suppresses the MEK/ERK pathway and ITGB4 in pancreatic cancer. *Oncotarget*. 2016;7(17):24719–24733. doi:10.18632/oncotarget.8348
15. Yang J, Huang Y, Song M, et al. SPC25 promotes proliferation and stemness of hepatocellular carcinoma cells via the DNA-PK/AKT/Notch1 signaling pathway. *Int J Biol Sci*. 2022;18(14):5241–5259. doi:10.7150/ijbs.71694

16. Ji H, Zhang JA, Liu H, Li K, Wang ZW, Zhu X. Comprehensive characterization of tumor microenvironment and m6A RNA methylation regulators and its effects on PD-L1 and immune infiltrates in cervical cancer. *Front Immunol*. 2022;13:976107. doi:10.3389/fimmu.2022.976107
17. Gies S, Melchior P, Molnar I, et al. PD-L1+ CD49f+ CD133+ circulating tumor cells predict outcome of patients with vulvar or cervical cancer after radio- and chemoradiotherapy. *J Transl Med*. 2025;23(1):321. doi:10.1186/s12967-025-06277-w
18. Xie M, Lin Z, Ji X, et al. FGF19/FGFR4-mediated elevation of ETV4 facilitates hepatocellular carcinoma metastasis by upregulating PD-L1 and CCL2. *J Hepatol*. 2023;79(1):109–125. doi:10.1016/j.jhep.2023.02.036
19. Chen C, Li S, Xue J, et al. PD-L1 tumor-intrinsic signaling and its therapeutic implication in triple-negative breast cancer. *JCI Insight*. 2021;6(8):e131458. doi:10.1172/jci.insight.131458
20. Tang W, Chen Z, Zhang W, et al. The mechanisms of sorafenib resistance in hepatocellular carcinoma: theoretical basis and therapeutic aspects. *Signal Transduct Target Ther*. 2020;5(1):87. doi:10.1038/s41392-020-0187-x
21. Wang S, Wang Y, Xun X, et al. Hedgehog signaling promotes sorafenib resistance in hepatocellular carcinoma patient-derived organoids. *J Exp Clin Cancer Res*. 2020;39(1):22. doi:10.1186/s13046-020-1523-2
22. Cheng Z, Wei-Qi J, Jin D. New insights on sorafenib resistance in liver cancer with correlation of individualized therapy. *Biochim Biophys Acta Rev Cancer*. 2020;1874(1):188382. doi:10.1016/j.bbcan.2020.188382
23. Guo L, Hu C, Yao M, Han G. Mechanism of sorafenib resistance associated with ferroptosis in HCC. *Front Pharmacol*. 2023;14:1207496. doi:10.3389/fphar.2023.1207496
24. Rimassa L, Finn RS, Sangro B. Combination immunotherapy for hepatocellular carcinoma. *J Hepatol*. 2023;79(2):506–515. doi:10.1016/j.jhep.2023.03.003
25. Xu R, Liu X, Li A, et al. c-Met up-regulates the expression of PD-L1 through MAPK/NF-κBp65 pathway. *J Mol Med*. 2022;100(4):585–598. doi:10.1007/s00109-022-02179-2
26. Yuan H, Xu R, Li S, et al. The malignant transformation of viral hepatitis to hepatocellular carcinoma: mechanisms and interventions. *MedComm*. 2025;6(3):e70121. doi:10.1002/mco2.70121
27. Chulkina M, Beswick EJ, Pinchuk IV. Role of PD-L1 in gut mucosa tolerance and chronic inflammation. *Int J Mol Sci*. 2020;21(23):9165. doi:10.3390/ijms21239165
28. Antonangeli F, Natalini A, Garassino MC, Sica A, Santoni A, Di Rosa F. Regulation of PD-L1 expression by NF-κB in cancer. *Front Immunol*. 2020;11:584626. doi:10.3389/fimmu.2020.584626
29. Lin KX, Istl AC, Quan D, Skaro A, Tang E, Zheng X. PD-1 and PD-L1 inhibitors in cold colorectal cancer: challenges and strategies. *Cancer Immunol Immunother*. 2023;72(12):3875–3893. doi:10.1007/s00262-023-03520-5
30. Ma SR, Liu JF, Jia R, Deng WW, Jia J. Identification of a favorable prognostic subgroup in oral squamous cell carcinoma: characterization of ITGB4/PD-L1high with CD8/PD-1high. *Biomolecules*. 2023;13(6):1014. doi:10.3390/biom13061014
31. Zhao M, Yuan H, Yang G, et al. Tumour cell-expressed PD-L1 reprograms lipid metabolism via EGFR/ITGB4/SREBP1c signalling in liver cancer. *JHEP Rep*. 2024;6(4):101009.
32. Wei Y, Wang Y, Liu N, et al. A FAK inhibitor boosts anti-PD1 immunotherapy in a hepatocellular carcinoma mouse model. *Front Pharmacol*. 2022;12:820446.
33. Ji HF, Yang ZQ, Han JJ, et al. Safflower yellow inhibits progression of hepatocellular carcinoma by modulating immunological tolerance via FAK pathway. *Chin J Integr Med*. 2024;30(4):339–347.
34. Zhang Y, Liang J, Cao N, et al. ASIC1α up-regulates MMP-2/9 expression to enhance mobility and proliferation of liver cancer cells via the PI3K/AKT/mTOR pathway. *BMC Cancer*. 2022;22(1):778.
35. Tian LY, Smit DJ, Jücker M. The role of PI3K/AKT/mTOR signaling in hepatocellular carcinoma metabolism. *Int J Mol Sci*. 2023;24(3):2652.
36. Zhu MX, Wei CY, Zhang PF, et al. Elevated TRIP13 drives the AKT/mTOR pathway to induce the progression of hepatocellular carcinoma via interacting with ACTN4. *J Exp Clin Cancer Res*. 2019;38(1):409. doi:10.1186/s13046-019-1401-y
37. Huang WY, Liao ZB, Zhang JC, et al. USF2-mediated upregulation of TXNRD1 contributes to hepatocellular carcinoma progression by activating Akt/mTOR signaling. *Cell Death Dis*. 2022;13(11):917. doi:10.1038/s41419-022-05363-x